Monte Carlo simulations of electrical percolation in multicomponent thin films with nanofillers

IOP Publishing Nanotechnology
Nanotechnology 29 (2018) 075401 (10pp) https://doi.org/10.1088/1361-6528/aaa0be

Monte Carlo simulations of electrical percolation in multicomponent thin films with nanofillers

Xiaojuan Ni[1], Chao Hui[1], Ninghai Su[1], Wei Jiang[1] and Feng Liu[1,2]

[1] Department of Materials Science and Engineering, University of Utah, Salt Lake City, UT 84112, United States of America
[2] Collaborative Innovation Center of Quantum Matter, Beijing, 100084, People's Republic of China

E-mail: fliu@eng.utah.edu

Received 1 September 2017, revised 5 December 2017
Accepted for publication 11 December 2017
Published 11 January 2018

Abstract

We developed a 2D disk–stick percolation model to investigate the electrical percolation behavior of an insulating thin film reinforced with 1D and 2D conductive nanofillers via Monte Carlo simulation. Numerical predictions of the percolation threshold in single component thin films showed good agreement with the previous published work, validating our model for investigating the characteristics of the percolation phenomena. Parametric studies of size effect, i.e., length of 1D nanofiller and diameter of 2D nanofiller, were carried out to predict the electrical percolation threshold for hybrid systems. The relationships between the nanofillers in two hybrid systems was established, which showed differences from previous linear assumption. The effective electrical conductance was evaluated through Kirchhoff's current law by transforming it into a resistor network. The equivalent resistance was obtained from the distribution of nodal voltages by solving a system of linear equations with a Gaussian elimination method. We examined the effects of stick length, relative concentration, and contact patterns of 1D/2D inclusions on electrical performance. One novel aspect of our study is its ability to investigate the effective conductance of nanocomposites as a function of relative concentrations, which shows there is a synergistic effect when nanofillers with different dimensionalities combine properly. Our work provides an important theoretical basis for designing the conductive networks and predicting the percolation properties of multicomponent nanocomposites.

Keywords: multicomponent nanocomposites, electrical percolation, carbon nanotubes, graphene nanoplatelets

(Some figures may appear in colour only in the online journal)

1. Introduction

The development of electrically conductive nanofillers and associated low-cost fabrication techniques have stimulated considerable interest in employing such materials to render electrically insulating nanocomposites conductive. Recent demonstrations of thin films incorporating 1D, e.g., carbon nanotubes (CNTs) [1, 2] and metal nanowires [3] and 2D e.g., graphene nanoplatelets (GNPs) conductive nanofillers [4], with promising applications in electronics, photovoltaic devices, and sensors, have motivated increasing efforts in experimental research [5–7]. Polymeric thin film containing conductive nanofiller exhibit a transition from insulating to conductive nature when the filler concentration exceeds the so-called percolation threshold, which characterizes a dramatic enhancement in electrical conductance. It is commonly believed that 1D and 2D conductive nanofillers can form cosupporting networks in which the 1D nanofillers act as long distance charge transporters while the 2D nanofillers serve as interconnections between 1D nanofillers by forming local conductive paths [8, 9]. Polymeric nanocomposites reinforced with carbon-based nanomaterials have been the subject of

intense experimental and theoretical study [10–15]. As shown by the experimental results, the hybrid composites cannot only combine the advantages of different nanofillers but also improve materials properties through a synergistic effect. Safdari *et al* confirmed the presence of the synergistic effect of electrical properties in hybrid ternary polymeric nanocomposites based on CNTs and GNPs, which outperform their single-filler counterpart configurations owing to the formation of a hybrid CNT/GNP network [11].

However, these experimental investigations were often conducted on a trial and error basis without a comprehensive understanding of the electrical percolation mechanisms in multicomponent nanocomposites. The percolation threshold studies have only been systematically carried out in discrete [16, 17] and continuum systems [18, 19] with a single component. To date, there have been only some limited efforts in simulating electrical percolation in multicomponent nanocomposite systems. For example, a sublinear relationship between CNTs and carbon black (CB) was shown by Chen *et al* [20]. A group of CB particles was equivalent to a hypothetical sphere with 30 vol% of conductive CB and 70 vol% of insulating polymeric matrix, which undoubtedly underestimated the percolation threshold since the insulating polymer matrix was considered to be conductive. A discrete model describing the electrical percolation of mixed CNTs and CB was proposed on the basis of the excluded volume theory [21, 22]. However, CNTs overlap with each other and can hardly be dispersed separately in experiments [23–25]. These works have two things in common: there are some constraints in their models in studying the percolation properties and the electrical conductance has not been evaluated in multicomponent systems.

Modeling of the electrical percolation properties of these multicomponent nanocomposites can provide general guidance for designing conductive networks reinforced with multiple nanofillers and understanding the phase transition at the percolation threshold. The aim of this study is to investigate the percolation phenomena by first removing the above mentioned constraints in 2D multicomponent thin films. We developed a disk–stick percolation model for the prediction of the electrical percolation threshold in multicomponent thin films via Monte Carlo simulations. With the assumption of a uniformly generated random dispersion of nanofillers, the present statistical model is able to predict the percolation threshold for a thin film incorporating multicomponent conductive nanofillers. The effects of lattice size, filler dimensions, relative concentration, and contact patterns on electrical performance were numerically examined and the enhancement of electrical performance in multicomponent thin films was confirmed by our resistor network model. In this study, we focus on 1D nanofillers, such as CNTs with a very high aspect ratio of length-to-diameter and 2D nanofillers, such as graphene flakes with a very high aspect ratio of area-to-thickness. However, our model is also applicable beyond nanofillers to micro- or macro-fillers with similar very large aspect ratios. In principle, given the similar aspect ratio, we expect the percolation threshold is size scalable.

2. Simulation procedure

2.1. Statistical disk model

A representative polymeric nanocomposite film of dimension $L \times L$ is occupied by disks with a uniformly generated random distribution. Disks with radius r are randomly dispersed in each lattice site with a given density, D_d (number of disks per unit area). Two random half-integer numbers within (0, L) were generated to establish the coordinates of the disk center in discrete model (see figure 1(a)). Similarly, as shown in figure 1(c), two random numbers within (0, L) were generated to establish the coordinates of the disk center in continuum model. The intersection of two disks is determined by the distance between them, d_{d-d}. The value of d_{d-d} is calculated by equation (1) if one disk is located within the subcell of the other. The dashed circle with $2 \times r$ as the radius in figure 2(a) is the subcell of the reference disk, depicted by equation (2).

$$d_{d-d} = \sqrt{(x_{dj} - x_{di})^2 + (y_{dj} - y_{di})^2} \quad (1)$$

$$(x - x_{di})^2 + (y - y_{di})^2 = (2\mathrm{r})^2 \quad (2)$$

It is explicitly shown in figure 2 that the tested disk is impossible to intersect the reference disk when its center is beyond the subcell. Two disks are connected once $d_{d-d} \leqslant 2 \times r$. A label is assigned to an individual disk after the determination of intersection. If the disk has zero connected neighbors, a new label will be given to it. If the disk has one connected neighbor, it will have the same label as its neighbor. Furthermore, if these neighboring disks have different labels and they correspond to the same cluster, the highest-numbered label is chosen as the cluster label and the neighboring disks will be reassigned a new label. The system percolates when its left and right boundaries are connected by a cluster consisting of disks with the same label. After 100 repetitions, the percolation probability was obtained by counting the times the system is percolated. The probability distribution function (PDF) is defined as the first-order derivative of the percolation probability and the percolation threshold is obtained by fitting the PDF with a Gaussian distribution function.

2.2. Statistical stick model

For the stick percolation model, a representative lattice of dimension $L \times L$ is occupied by sticks with a uniformly generated random distribution, as shown in figure 1(b). The widthless sticks with length $= l$ are randomly dispersed in the lattice with a given density, Ds (number of sticks per unit area). A stick is generated by the random coordinates (x_s, y_s) for its center and a random angle θ with respect to the vertical direction for its orientation. (Note that $0 < x_s < L$, $0 < y_s < L$, and $0 \leqslant \theta \leqslant \pi$). The intersection point (x_j, y_j) of the two sticks is obtained by solving the linear equations if one stick is located within the subcell of the other. The subcell of the stick in figure 2(b) is described by equation (3). Two sticks are in contact if the intersection point is located within both of the stick segments. This method is highly convenient and simple due to the use of local coordinates and angles. The labeling process and

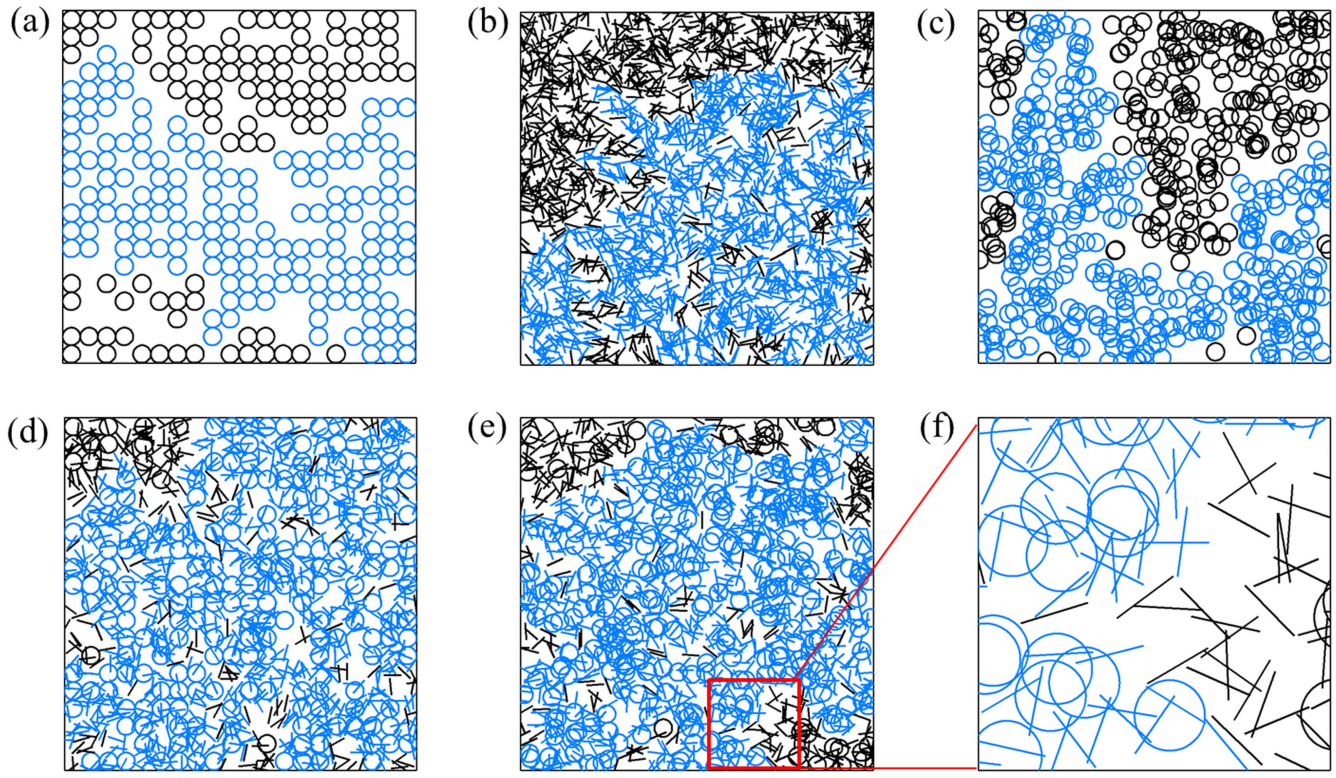

Figure 1. Graphic representations of the (a) discrete disk, (b) continuum stick, (c) continuum disk, and hybrid systems (I) (d) and (II) (e). By zooming in on the red region, (f) shows clearly that black fillers are distributed separately from the blue percolating cluster.

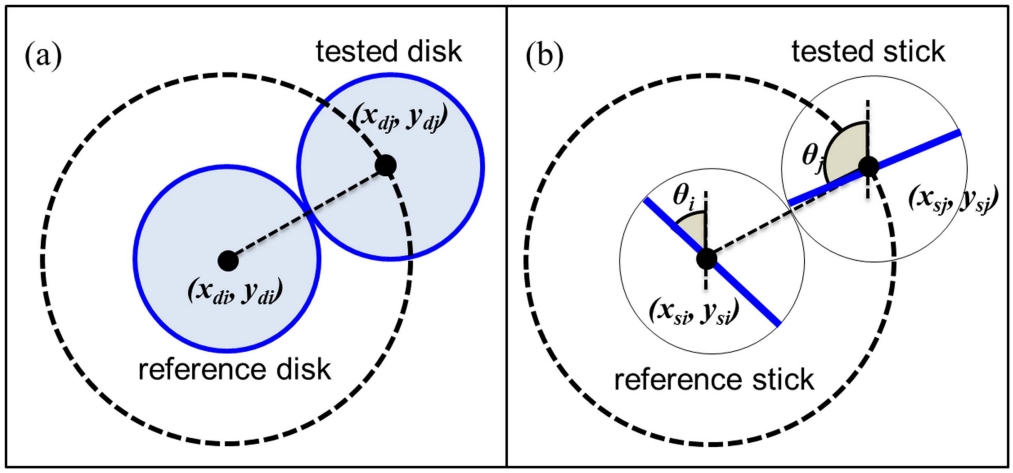

Figure 2. Schematic illustrations of subcells in the disk percolation model (a) and stick percolation model (b).

percolation probability calculation are the same as described in section 2.1. It should be noticed that the 1D nanofillers simulated as sticks are not penetrable to each other in the actual thin films, and they are assumed to superpose on each other in our simulation. The curvature effect of 1D nanofiller was not considered in this study. Even though the curved shape of 1D nanofiller can lead to lower electrical conductance compared with straight one, the effect is very limited [14, 26].

$$(x - x_{si})^2 + (y - y_{si})^2 = l^2 \quad (3)$$

2.3. Statistical stick-disk model

In order to evaluate the percolation thresholds at different combinations of 1D sticks and 2D disks, a hybrid system (I) was generated by discrete disks and continuum sticks and a hybrid system (II) was formed by continuum disks and sticks, which are represented in figures 1(d) and (e), respectively. There are three contact patterns between the disk and stick according to the number of intersection points. Firstly, we find the points of the intersection given by the disk defined by the center and radius, and a line defined by the slope and

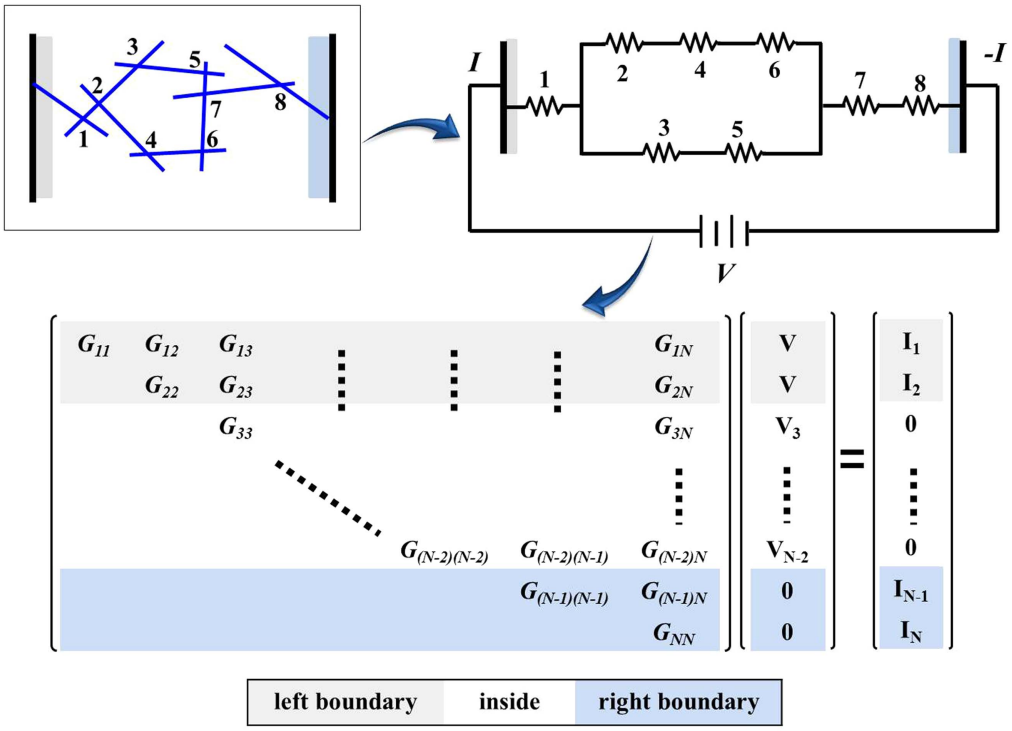

Figure 3. Stick percolation model, the corresponding resistor network. and the general conductance matrix.

y-intercept, which contains the stick. A disk and a stick are in contact if they both satisfy two conditions: (1) the intersection points exist; (2) the distance between one of the intersection points and the stick center is less than half length of the stick. The labeling process and percolation probability calculation are the same as described in section 2.1.

2.4. Resistor network model

The conductive 1D/2D hybrid system can be transformed into a resistor network. Conductive nanofillers are assumed to have no electrical resistance and the junction point of two nanofillers is assumed to be a resistor in the equivalent circuit. The equipotential nanofiller is reduced to a node in the resistor network. Based on the well-known matrix representation for a resistor network and Kirchhoff's current law (KCL), as shown in figure 3, the total current I under an applied voltage can be estimated [27, 28]. For those nanofillers that are connected to the left boundary, the sum of the currents is equal to I, and for those connected to the right boundary, the sum of the current is equal to –I, and for those within the matrix, the current is zero. From the above conditions and KCL, we obtained a large-scale linear algebraic equation system, which can be written in a matrix form:

$$G[N \times N] \cdot V[N \times 1] = I[N \times 1]. \quad (4)$$

N is the total number of nanofillers in the percolating cluster. Since the voltage applied from left to right across the network is arbitrarily set to 1 V, the $N \times N$ matrix can be reduced to an (N-N_{left}-N_{right}) $\times$ (N-N_{left}-N_{right}) matrix. N_{left} and N_{right} are the numbers of nanofillers that are connected to the left and right boundaries, respectively. Nodal voltage V_i is obtained by computing the inverse matrix of G through the Gaussian elimination method, from which the equivalent resistance and conductance are obtained. Finally, the total current I is evaluated following Ohm's law, $I = G \times (V_{\text{left}} - V_{\text{right}})$.

3. Results and discussion

3.1. Percolation in single component thin films

The computational code for the Monte Carlo simulations was developed in Matlab to numerically investigate the percolation properties in thin films reinforced with 1D and 2D conductive nanofillers. The results of the percolation probability for the disk system and stick system of a variety of lattice sizes in the vicinity of the percolation transition are shown in figure 4. The percolation probability was calculated as the ratio of the successfully percolated times over the total number of simulations performed. The percolation threshold is expected to be a sudden increase in percolation probability from the theory, while as shown in figures 4(a), (c) and (e), a smooth increase in percolation probability is seen instead due to the finite lattice size being simulated. The rate of convergence is determined by two factors. The first comes from the width of the critical region, which is the full width at half maximum (FWHM). FWHM scales as $L^{-1/\upsilon}$, where $\upsilon = 4/3$ is the universal critical exponent for 2D percolation. The second factor is the rate of convergence of the percolation probability to its asymptotic value in an infinite lattice, which can be represented by the PDF. In a finite lattice, PDF cannot diverge but reaches the maximum of a finite height. Both FWHM and the magnitude of the height depend on the lattice size. Percolation thresholds can be easily read from the intersection points of the percolation probability curves,

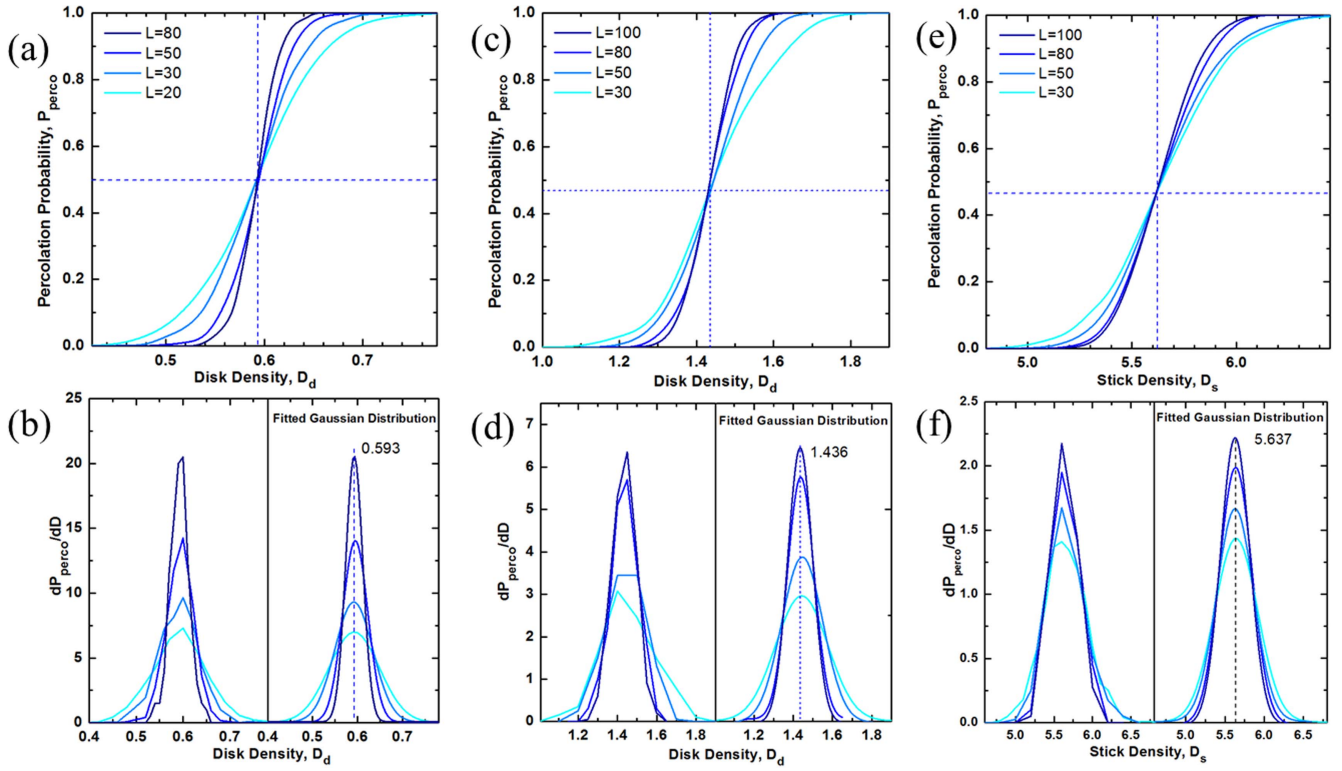

Figure 4. (a), (b) Discrete disk model; (c), (d) continuum disk model; (e), (f) continuum stick model. (a), (c), (e) Percolation probability as a function of lattice size; (b), (d), (f) percolation threshold obtained with PDF. The dashed lines denote the expected percolation threshold.

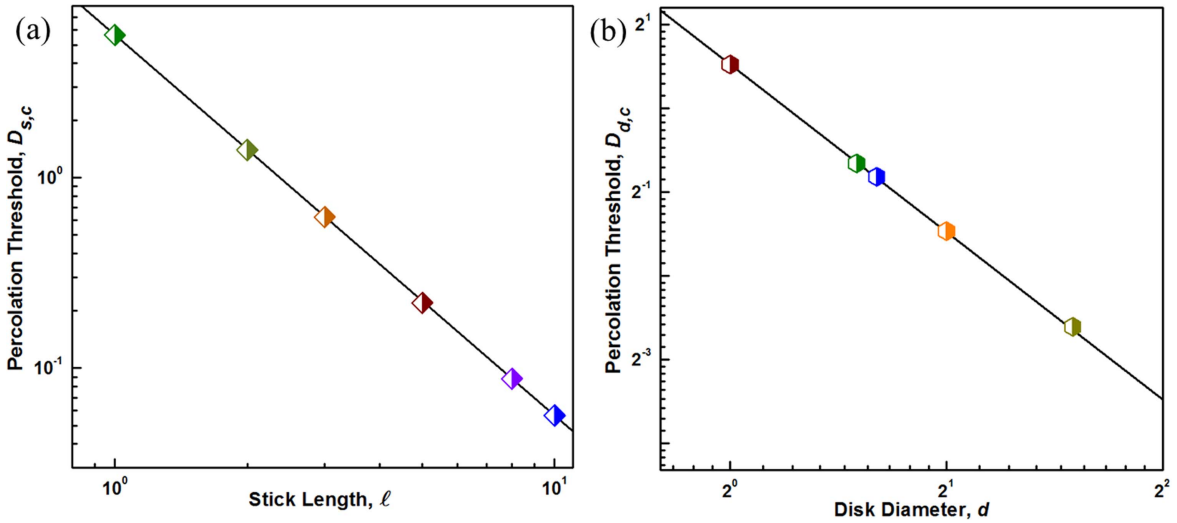

Figure 5. Percolation threshold as a function of nanofiller size in continuum stick model (a) with $\log(D_{s,c}) = \log(5.637) - 2 \times \log(l)$, and continuum disk model (b) with $\log(D_{d,c}) = \log(1.436) - 2 \times \log(d)$.

which are 0.593, 1.428, and 5.637, respectively, exhibiting good agreement with previously published results [18, 19, 29]. Also, the percolation threshold corresponds to the maximum in the PDF, shown in figures 4(b), (d), and (f), which provides an alternative method to obtain the percolation threshold without simulating multiple lattice sizes.

The size of the nanofiller plays an important role in determining the percolation threshold in thin films. It is obvious that $D_c \propto d^{-2}$ applies to discrete disk model. Hence a straight line is expected if $\log(D_c)$ is plotted versus $\log(l^{-2})$ or $\log(d^{-2})$ in continuum models, and this is exactly what we observed in figure 5. The straight line with slope -2 suggests that there is an inverse parabolic relationship between the percolation threshold and the size of the nanofillers in continuum models. The effect of the nanofiller's size in hybrid systems will be further described. Our predictions of the percolation threshold in thin films of a single nanofiller with discrete and continuum distributions and the effect on the percolation threshold from the size of fillers are consistent with previous published work [18, 19, 29], which give a solid

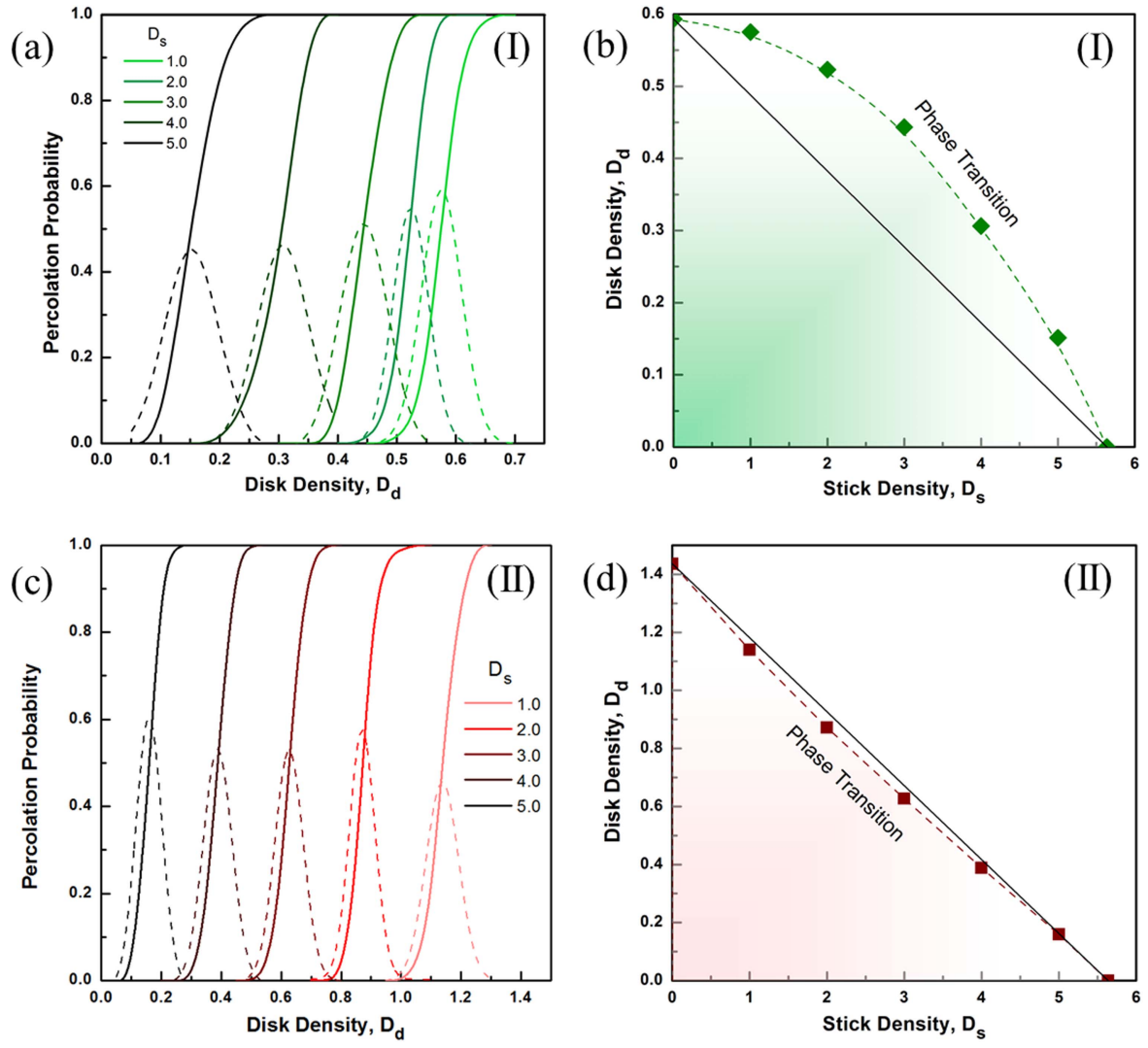

Figure 6. (a), (c) Effect of stick density on the percolation probability; (b), (d) relationships between the densities of the nanofillers at the percolation threshold in hybrid system (I) and hybrid system (II).

theoretical basis for the investigation of percolation phenomena in multicomponent hybrid systems (I) and (II).

3.2. Percolation in multicomponent thin films

When the thin films are incorporated with multicomponent nanofillers, the main question is how the density leading to the phase transition from the insulator to the conductor changes compared with single component systems. Figures 6(a) and (c) show the percolation probability in hybrid systems, which have already been occupied by a certain density of stick. The PDF for each stick density was represented by the dashed lines, from which we can read the critical density of the disk. The superlinear relationship in (I) and sublinear relationship in (II) between the densities of the 1D and 2D nanofillers at the percolation threshold were established in figures 6(b) and (d). The relationships are different from the previous linear assumption [21, 22], in which both the CNTs and CB are with discrete distributions. Generally, the percolation threshold depends on the dimensions of nanofillers. The effect of the nanofiller's size in hybrid systems at the percolation threshold is represented in table 1, and it explicitly shows how the density of the disk decreases with the increasing of the length of stick in both hybrid systems (I) and (II) with Ds = 1. The effect of size on the percolation properties can shed some light on how one can maximize the percolation probability and how one can tailor

Table 1. The relationships between the disk and the stick at the percolation threshold with different lengths of sticks in hybrid system (I) and hybrid system (II) with Ds = 1.

Stick length	$D_{d,c}$[a] in (I)	$D_{d,c}$[a] in (II)
1.0	0.575 ± 0.001	1.140 ± 0.002
1.2	0.541 ± 0.002	1.003 ± 0.004
1.4	0.510 ± 0.001	0.866 ± 0.002
1.6	0.453 ± 0.001	0.722 ± 0.005
1.8	0.374 ± 0.001	0.545 ± 0.004
2.0	0.273 ± 0.002	0.365 ± 0.003

[a] $D_{d,c}$ is the critical density of disk at the percolation threshold.

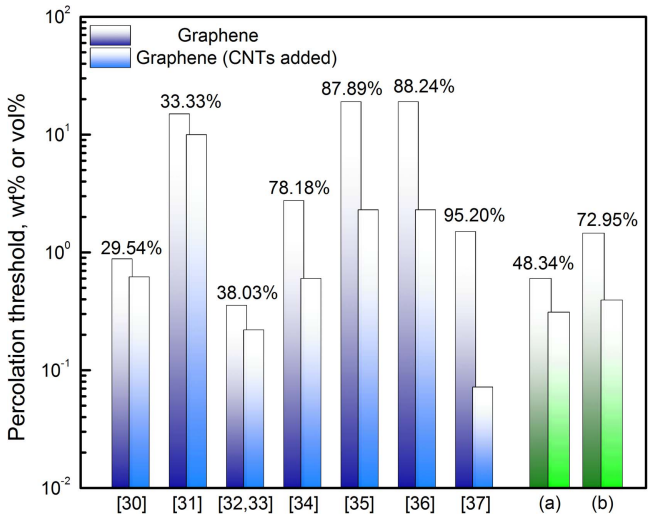

Figure 7. Comparison between the experimental studies ([30–37]) and our simulation results ((a) and (b)). (a) is the hybrid system (I) and (b) is the hybrid system (II) with Ds = 4. The percentage indicates the decrease in the electrical percolation threshold of the graphene after adding CNTs.

the size of the nanofillers to minimize the mass consumption in multicomponent thin films.

A comparison of the simulation results with the experimental ones is shown in figure 7 [30–37]. It clearly shows that there is a substantial drop in the percolation threshold of graphene ranging from 29.5%–95.2% after adding CNTs into the nanocomposites depending on the experimental setup, which is consistent with the simulation results of a 48.34% and 72.95% reduced threshold of the 2D nanofillers for the hybrid systems (I) and (II), respectively. The actual percentage drop in the threshold of the 2D nanofillers is adjustable by regulating the size of the nanofillers in the percolation model. Thus, the comparison between the experimental results and our simulations has qualitatively validated our model.

3.3. Electrical performance

The KCL and Gaussian elimination methods were used to calculate the distribution of the nodal voltage. Distributions of voltage in three cases are illustrated in figure 8, and the voltage decreases throughout the network as expected. We did not include the resistance of the nanofiller in our calculation, since it is on the order of 10^{-2} times smaller than the junction resistance [38, 39]. In the percolation threshold study, the lattice size has a significant influence on the convergence and accuracy of the calculations. In contrast, as shown in figure 9, the lattice size has a negligible effect on the electrical conductance for both the disk and stick models, which suggests that the electrical conductance is independent of lattice size. The lattice size used to investigate the electrical conductance is 10 × 10, which will significantly reduce the computational time while at the same time maintain the accuracy of the evaluations. The conductance exponent we derived as $t \approx 1.36$ is in good agreement with the universal value of 1.30 for lattice percolation [40, 41].

In our simulation, each junction of two nanofillers is modeled by an effective contact resistance. The resistance of the stick–stick is assumed to be five times larger than that of the disk–disk owing to the contact area of the disk–disk is larger than that of the stick–stick, which is the point contact. The mass ratio of the disk to stick and the length of the stick were also taken into account. Generally, the mass of disk is at least ten times heavier than that of the stick and eight different mass ratios were evaluated, as shown in figure 10(a). It is obvious that the conductance increases with the increasing of the mass ratio since more sticks were introduced to form the conductive network with more junctions and hence leading to a reduced equivalent resistance. The effect of length on the electrical conductance is the same as that of the mass ratio (figure 10(b)). There are 2862 ± 47, $11\,370 \pm 95$ and $24\,125 \pm 230$ intersection points for length = 1, 2, and 3 with Ds = 7 on a 10 × 10 lattice, respectively. The variation in conductance with a convex shape, shown in figures 10(a) and (b) suggests that the nanocomposites incorporating 1D and 2D nanofillers exhibit a significant synergistic effect when nanofillers with different dimensionalities are properly combined, which is consistent with the experimental observations [30, 33, 36, 42, 43]. The enhancement of the electrical conductivity in the hybrid nanocomposites is mainly due to the increased formation of multiple junctions between the nanofillers. All the junctions of the disk–disk, disk–stick, and stick–stick contribute to the effective conductance of the nanocomposites. Compared with the specific distribution of the individual junction shown in figure 10(c), only the heterojunction of the stick–disk shows a convex shape with respect to the concentration, which indicates that the number of the stick–disk heterojunction is the dominant factor in enhancing the overall electrical performance of the hybrid nanocomposites due to the higher conductance generated by the larger contact area between the disk and stick compared with the point contact of the stick–stick and non-overlaying disk–disk junctions. The mechanism of the contact resistance between the overlapped disks is not clear so far, therefore, we did not evaluate the electrical properties in hybrid system (II).

The predictions of electrical percolation threshold in multicomponent nanocomposites have been validated through a comparison between the experimental results and our simulation ones, as shown in figure 7. Since there is a large range of variations in the experimental data depending on the experimental setups and conditions, a more detailed comparison might be conducted in the future by performing simulations with parameters that match closer to the specific experimental conditions for a more direct and quantitative comparison. This may provide useful guidelines for future experiments. Furthermore, in addition to the electrical percolation prediction, our model should be extendable to studying other properties of nanocomposites in relation to the percolation threshold. For instance, the optimal nanomaterials concentration (ONC) yielding a maximal reinforcement in fracture toughness has been experimentally studied by Nadiv *et al* for composites reinforced by 1D CNTs, tungsten nanotubes (WS2NT), and 2D graphene nanoribbons (GNR) [44]. The ONC is typically located in the vicinity of the

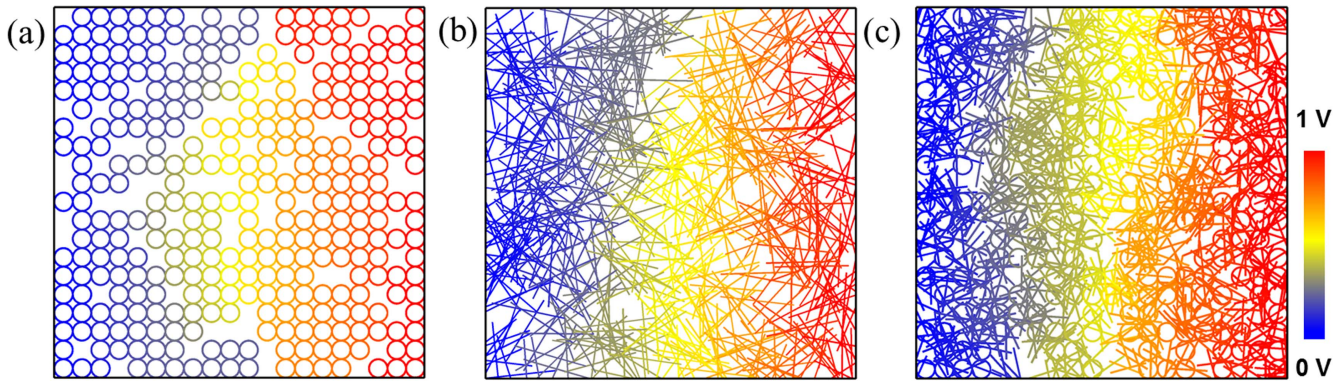

Figure 8. Distribution of the nodal voltage in the disk system with $D_d = 0.8$ (a), stick system with $D_s = 7$ (b) and hybrid system (I) with $D_d = 0.6$ and $D_s = 2.8$ (c). The left boundary voltage is 0 V and right boundary voltage is 1 V, the red and blue colors in the color bar indicate 1 V and 0 V, respectively. The density of the nanofillers is much higher than the percolation threshold.

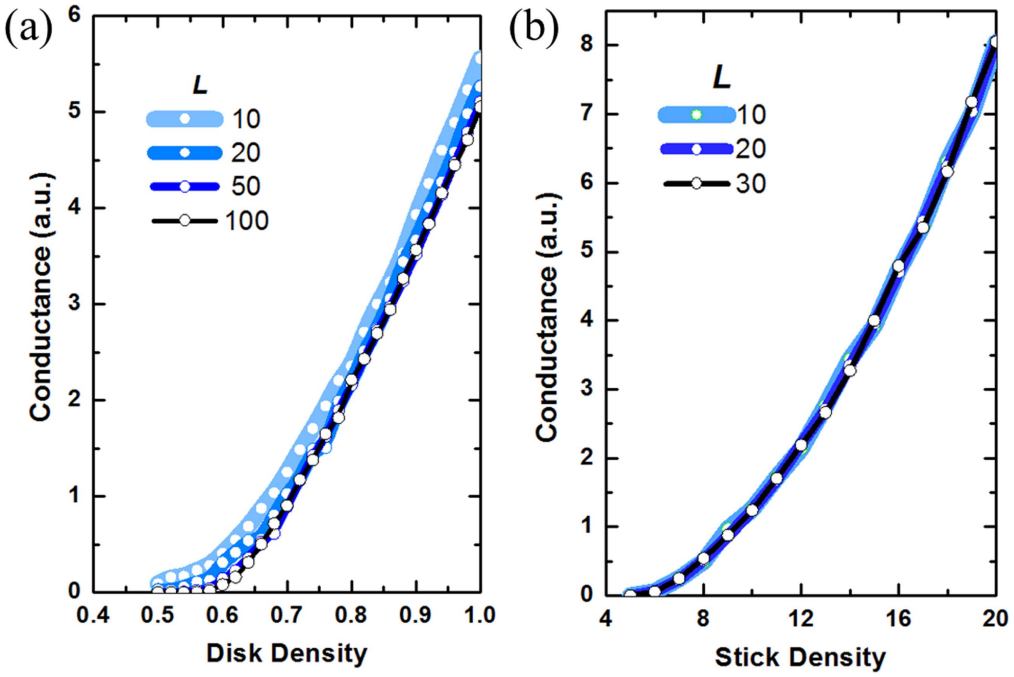

Figure 9. Electrical conductance as a function of lattice size in the disk (a) and stick (b) systems.

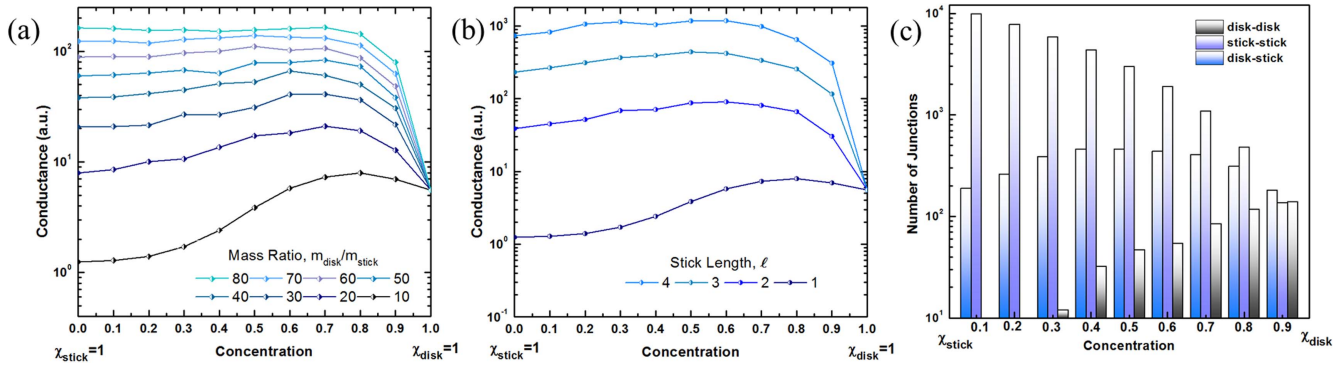

Figure 10. Electrical conductance diagram with respect to: (a) mass ratio of the disk to stick; (b) stick length; and (c) distribution of the junction number in hybrid system (I).

rheological percolation threshold, which characterizes the sudden change in the viscosity of the nanocomposite. It is not necessary for the nanofillers to contact each other at the rheological percolation threshold. Therefore, by adjusting the intersection determination on the shortest distance between the nanofillers, our model is applicable to predict the rheological percolation threshold and to further elucidate their experimental observations on ONC. Further work will be carried out to help interpret the synergistic effect in complex hybrid systems and study the percolation phenomena in 3D multicomponent nanocomposite systems.

4. Conclusions

A 2D disk–stick model describing the electrical percolation behavior in nanocomposites incorporating 1D and 2D conductive nanofillers is proposed on the basis of a Monte Carlo simulation. The electrical percolation behavior in the vicinity of the percolation transition has been numerically investigated and the electrical percolation thresholds have been successfully predicted. Our model is able to estimate the critical density of nanofillers at the percolation threshold in multicomponent nanocomposite systems. It is capable of generating a microstructure with a specified density of nanofillers and adjusting several parameters such as the size of the lattice and the dimensions of the nanofillers. This computational methodology can be used as an aid in studying the percolation phenomena of polymeric thin films with multiple nanofillers.

Acknowledgments

This work is supported by U.S. DOE-BES (Grant No DE-FG02–04ER46148) and the Life-E company in Salt Lake City, UT. We also acknowledge the support from DOE-NERSC and CHPC at the University of Utah for providing the computing resources.

ORCID iDs

Xiaojuan Ni https://orcid.org/0000-0002-5845-7404

References

[1] Geier M L, McMorrow J J, Xu W, Zhu J, Kim C H, Marks T J and Hersam M C 2015 Solution-processed carbon nanotube thin-film complementary static random access memory *Nat. Nanotechnol.* **10** 944–8
[2] Zare Y and Yop K 2017 The mechanical behavior of CNT reinforced nanocomposites assuming imperfect interfacial bonding between matrix and nanoparticles and percolation of interphase regions *Compos. Sci. Technol.* **144** 18–25
[3] Gelves G A, Lin B, Sundararaj U and Haber J A 2008 Electrical and rheological percolation of polymer nanocomposites prepared with functionalized copper nanowires *Nanotechnology* **19** 12
[4] Fan P, Wang L, Yang J, Chen F and Zhong M 2012 Graphene/poly (vinylidene fluoride) composites with high dielectric constant and low percolation threshold *Nanotechnology* **23** 8
[5] Park S, Vosguerichian M and Bao Z 2013 A review of fabrication and applications of carbon nanotube film-based flexible electronics *Nanoscale* **5** 1727–52
[6] Maarouf A A, Kasry A, Chandra B and Martyna G J 2016 A graphene–carbon nanotube hybrid material for photovoltaic applications *Carbon* **102** 74–80
[7] Zein A E, Huppe C and Cochrane C 2017 Development of a flexible strain sensor based on PEDOT:PSS for thin film structures *Sensors* **17** 1337
[8] Thongruang W, Spontak R J and Balik C M 2002 Bridged double percolation in conductive polymer composites: an electrical conductivity, morphology and mechanical property study *Polymer* **43** 3717–25
[9] Clingerman M L, Weber E H and King J A 2002 Synergistic effects of carbon fillers in electrically conductive nylon 6,6 and polycarbonate based resins *Polymer* **23** 911–24
[10] Simoes R, Silva J, Vaia R, Sencadas V, Costa P, Gomes J and Senentxu L-M 2009 Low percolation transitions in carbon nanotube networks dispersed in a polymer matrix: dielectric properties, simulations and experiments *Nanotechnology* **20** 8
[11] Safdari M and Al-Haik M S 2013 Synergistic electrical and thermal transport properties of hybrid polymeric nanocomposites based on carbon nanotubes and graphite nanoplatelets *Carbon* **64** 111–21
[12] Wu X, Qi S, He J and Duan G 2010 High conductivity and low percolation threshold in polyaniline/graphite nanosheets composites *J. Mater. Sci.* **45** 483–9
[13] Li J, Li X, Fan C, Yao H, Chen X and Liu Y 2017 Study on the preparation of a high-efficiency carbon fiber dissipating coating *Coatings* **7** 1–11
[14] Hu N, Masuda Z, Yan C, Yamamoto G, Fukunaga H and Hashida T 2008 The electrical properties of polymer nanocomposites with carbon nanotube fillers *Nanotechnology* **19** 215701
[15] Xu S, Rezvanian O, Peters K and Zikry M A 2013 The viability and limitations of percolation theory in modeling the electrical behavior of carbon nanotube–polymer composites *Nanotechnology* **24** 7
[16] Ziff R M 1992 Spanning probability in 2D percolation *Phys. Rev. Lett.* **69** 2670–3
[17] Newman M E J and Ziff R M 2000 Efficient Monte Carlo algorithm and high-precision results for percolation *Phys. Rev. Lett.* **85** 4104–7
[18] Mertens S and Moore C 2012 Continuum percolation thresholds in two dimensions *Phys. Rev.* E **6** 1–6
[19] Li J and Zhang S L 2009 Finite-size scaling in stick percolation *Phys. Rev.* E **80** 1–4
[20] Chen Y, Wang S, Pan F and Zhang J 2014 A numerical study on electrical percolation of polymer matrix composites with hybrid fillers of carbon nanotubes and carbon black *J. Nanomater.* **86** 1–9
[21] Sun Y, Bao H D, Guo Z X and Yu J 2009 Modeling of the electrical percolation of mixed carbon fillers in polymer-based composites *Macromolecules* **42** 459–63
[22] Xiong Z Y, Zhang B Y, Wang L, Yu J and Guo Z X 2014 Modeling the electrical percolation of mixed carbon fillers in polymer blends *Carbon* **70** 233–40
[23] Hollertz R, Chatterjee S, Gutmann H, Geiger T, Nüesch F A and Chu B T T 2011 Improvement of toughness and electrical properties of epoxy composites with carbon nanotubes prepared by industrially relevant processes *Nanotechnology* **22** 125702
[24] McAndrew C F and Baxendale M 2013 High electrical conductance enhancement in Au-nanoparticle decorated sparse single-wall carbon nanotube networks *Nanotechnology* **24** 305202

[25] Mathieu B, Anthony C, Arnaud A and Lionel F 2015 CNT aggregation mechanisms probed by electrical and dielectric measurements *J. Mater. Chem.* C **3** 5769–74
[26] Soto M, Esteva M, Martínez-Romero O, Baez J and Elías-Zúñiga A 2015 Modeling percolation in polymer nanocomposites by stochastic microstructuring *Materials* **8** 6697–718
[27] Last B J and Thouless D J 1971 Percolation theory and electrical conductivity *Phys. Rev. Lett.* **27** 1719–21
[28] Balberg I, Binenbaum N and Anderson C H 1983 Critical behavior of the two-dimensional sticks system *Phys. Rev. Lett.* **51** 1605–8
[29] Newman M E J and Ziff R M 2001 Fast Monte Carlo algorithm for site or bond percolation *Phys. Rev.* E **64** 16706
[30] Yue L, Pircheraghi G, Monemian S A and Manas-zloczower I 2014 Epoxy composites with carbon nanotubes and graphene nanoplatelets-dispersion and synergy effects *Carbon* **78** 268–78
[31] Che J, Wu K, Lin Y, Wang K and Fu Q 2017 Largely improved thermal conductivity of HDPE/expanded graphite/carbon nanotubes ternary composites via filler network-network synergy *Compos. Part* A **99** 32–40
[32] Yin S, Rong C and Zhang S 2011 The preparation and electrical properties of the functionalized graphene/poly (ether sulfone) nanocomposites *High Peform. Polym.* **23** 592–601
[33] Zhang S, Yin S, Rong C, Huo P, Jiang Z and Wang G 2013 Synergistic effects of functionalized graphene and functionalized multi-walled carbon nanotubes on the electrical and mechanical properties of poly(ether sulfone) composites *Eur. Polym. J.* **49** 3125–34
[34] Oh J Y, Jun G H, Jin S, Ryu H J and Hong S H 2016 Enhanced electrical networks of stretchable conductors with small fraction of carbon nanotube/graphene hybrid fillers *Appl. Mater. Interfaces* **8** 3319–25
[35] Araby S, Saber N, Ma X, Kawashima N, Kang H and Shen H 2015 Implication of multi-walled carbon nanotubes on polymer/graphene composites *J. Mater.* **65** 690–9
[36] Liu H, Gao J, Huang W, Dai K, Zheng G, Liu C, Shen C, Yan X, Guo J and Guo Z 2016 Electrically conductive strain sensing polyurethane nanocomposites with synergistic carbon nanotubes and graphene bifillers *Nanoscale* **8** 12977–89
[37] Maiti S and Khatua B B 2016 Graphene nanoplate and multiwall carbon nanotube–embedded polycarbonate hybrid composites: high electromagnetic interference shielding with low percolation threshold *Polym. Compos.* **37** 2058–69
[38] Fuhrer M S *et al* 2000 Crossed nanotube junctions *Science* **288** 494–7
[39] Buldum A and Lu J P 2001 Contact resistance between carbon nanotubes *Phys. Rev.* B **63** 161403
[40] Li J and Zhang S-L 2010 Conductivity exponents in stick percolation *Phys. Rev.* E **1** 21120
[41] Stauffer D and Aharony A 2003 *Introduction to Percolation Theory* (London: Taylor and Francis)
[42] Lin J, Lin Z, Pan Y, Chen C, Huang C, Huang C and Lou C 2016 Improvement in mechanical properties and electromagnetic interference shielding effectiveness of PVA-Based composites : synergistic effect between graphene nanotubes *Macromol. Mater. Eng.* **301** 199–211
[43] Kumar S, Sun L L, Caceres S, Li B, Wood W, Perugini A, Maguire R G and Zhong W H 2010 Dynamic synergy of graphitic nanoplatelets and multi-walled carbon nanotubes in polyetherimide nanocomposites *Nanotechnology* **21** 1–9
[44] Nadiv R, Shtein M, Shachar G and Varenik M 2017 Optimal nanomaterial concentration: harnessing percolation theory to enhance polymer nanocomposite performance *Nanotechnology* **28** 305701